J. of Basic Sciences, Cheju Nat'l Univ
14(1), 17~22, 2001

기초과학연구 제주대학교
14(1), 17~22, 2001

Simulation of the Bursting Activity of Neuron R15 in Aplysia Kurodai

Nam Gyu Hyun, Yong Joo Kim and Young Hun Yu
Department of Physics, Cheju National University, Jeju 690-756

The object of this paper was to simulate the dynamic activity of Neuron R15 in the abdominal ganglion of Aplysia kurodai in a manner consistent with the data given to us by J. H. Han at the Molecular Neurobiology Laboratory at SNU, using Mathematica program. The model based on Ca^{2+} -blockable Ca^{2+} channel was used to simulate the activity of R15. Although the experimented and simulated results did not coincided exactly, we saw the possibility to have better results in the future. Membrane currents and the oscillation in the Ca^{2+} contributing to the electrical activity have been analysed.

I. INTRODUCTION

The R15 cell in the abdominal ganglion of Aplysia has been used to gain insights into the biophysical mechanism underlying bursting activity in nerve cells. Consequently, a good deal is known about the specific membrane currents.[1–4] In this paper, we wanted to simulate the time series of the bursting activity of neuron R15 in Aplysia kurodai recorded by J. H. Han at SNU. We accumulated a little information on Aplysia Kurodai in Section II. In section III, we reviewed the model based on the Ca^{2+}-blockable Ca^{2+} channel. [4] Section IV, contains results.

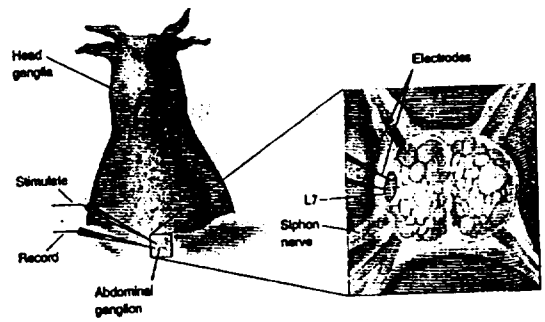

FIG. 1: a.The abdominal ganglion of aplysia kurodai.

II. APLYSIA KURODAI

Aplysia Kurodai are commonly found along the Eastern Asin Pacific coastal lines. Its nervous system was compared with that of Aplysia californica,[5] which has been well studied up to the levels of both behavior and cell biology. [6] We can catch some of Korean sea snail, Aplysia kurodai in Jeju coastal lines. We can also see the abdominal ganglion of Aplysia and a neuron R15 in Fig. 1 and 2 respectively. The neuron R15 in the abdominal ganglion of Aplysia kurodai fires regularly recurrent groups of action potentials, showing a bursting pattern. It was impaled with microelectrodes and their membrane potentials were recorded in the current clamp mode at the Molecular Neurobiology Laboratory in Seoul National University, and one of bursting pattern of them are Shown in Fig. 3.

III. MODEL

The model reviewed in this paper is based on the Ca^{2+} blockable Ca^{2+} channel model presented in Chay, Fan, and Lee. [4] This model contains four ionic currents - the fast inward current I_{fast}, the slow Ca^{2+} current I_{slow}, the delayed rectifying K^+ current I_K, and the leak current I_{leak}. There are six dynamic variables in this model. The first variable is membrane potential V which changes with time in the following form:

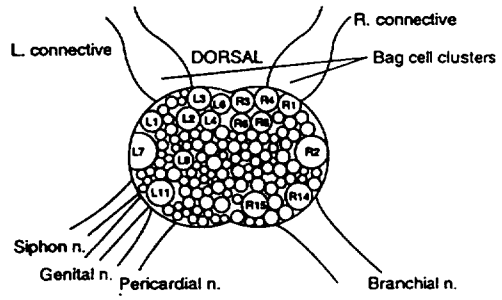

FIG. 2: The most common locations of the identified cells are shown on the dorsal sides of the ganglion.

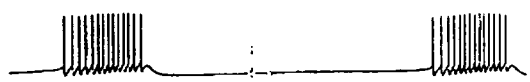

FIG. 3: A bursting pattern in the abdominal ganglion of Aplysia kurodai.

$$-C_m\frac{dV}{dt} = g_{fast}\, m_\infty h(V - V_{fast}) + g_{slow}\, d\, f(V - V_{slow}) + g_K\, n(V - V_K) + g_L(V - V_L). \quad (1)$$

Where g_{fast}, g_{slow}, g_K, and g_L are the maximal conductances of a fast inward current, a slow calcium current, a delayed rectifying K^+ current, and a leak current; V_{fast}, V_{slow}, V_K, and V_L are the reversal potentials for their respective currents; m and h are the activation and inactivation gating variables of the fast current(where m_∞ is the m at the steady state), d and f are the activation and inactivation of the slow inward current, and n is the opening probability of the outward current. Note that the Eq. (1) also contains four types of currents. In this model, the second term is responsible for the genesis of the slow underlying wave. The hypothesis in this model is that the Ca^{2+} channel becomes inactive when a Ca^{2+} ion binds to the receptor site located at the pore of the channel. Accordingly, its kinetic scheme may be represented as follows

$$BLOCKED \underset{\lambda_f C}{\overset{\lambda_f}{\rightleftharpoons}} UNBLOCKSED, \quad (2)$$

where $C = [Ca^{2+}]_i/K_{Ca}$, λ_f is the forward kinetic constant from the blocked state to the unblocked state, and K_{Ca} is the dissociation constant of the Ca^{2+} ion from its receptor site located in the pore of the Ca^{2+} channel. Then, the fraction of calcium channels which is unblocked, f, can be obtained from the above kinetic scheme as,

$$\frac{df}{dt} = \lambda_f(1 - f) - \lambda_f \frac{[Ca^{2+}]_i}{K_{Ca}} f. \quad (3)$$

In the modern view, f can be interpreted as the fraction of available Ca^{2+} channels at time t (instead of the inactivation variable). As $[Ca^{2+}]_i$ increases, the availability of functional Ca^{2+} channels decreases due to dephosphorylation by a calcium dependent protein. If the process described in Eq.(2) is fast (i.e., λ_f is large) then f can be approximated by its steady state value $f_\infty = 1/(1 + C)$. This is the expression used by others to describe the inactivation term of the Ca^{2+} channel, but as we show here it has a limited applicability. As in the Hodgkin-Huxley model, we assume that the three other gating variables h, d, and n depend on time and potential in such a way that

$$\frac{dy}{dt} = \frac{y_\infty - y}{\tau_y}, \quad y = h,\ d,\ \text{and } n, \quad (4)$$

where y_∞ and τ_y are the y at its steady state and relaxation constant, respectively. Here, the steady state expression takes the following form,

$$y_\infty = \frac{1}{1 + \exp(\frac{V_y - V}{S_y})}, \quad y = m,\ h,\ d, \text{and } n. \quad (5)$$

According to this model, the relaxation constants take the form

$$\tau_y = \frac{\tau_y^*}{1+\exp(a_y\frac{V_y-V}{S_y})+\exp((a_y-1)\frac{V_y-V}{S_y})},$$
$$y = h,\ d,\ \text{and}\ n, \qquad (6)$$

where V_y is the voltage at the half maximal point, S_y is the slope at $V = V_y$, τ_y^* is the maximal relaxation time constant, and a_y determines how the relaxation constant τ_y depends on voltage (for example, $a_y = 0.5$ makes τ_y a bell shape as an increasing function of V).

In the scheme shown by Eq. (2), $[Ca^{2+}]_i$ depends on the influx of Ca^{2+} from outside through the calcium channel and the efflux of Ca^{2+} via the Ca^{2+}-pump. This effect is expressed by the following mathematical expression:

$$\frac{dC}{dt} = \rho\{\frac{g_{slow}df(V_{slow}-V)}{\sigma} - k_{Ca}C + k_{Ca}C_r\},$$
$$C = \frac{[Ca^{2+}]_i}{K_{Ca}}, \qquad (7)$$

where ρ is a measure of the Ca^{2+} buffer capacity of the cell, and σ is the factor that converts the electromotive force to the concentration gradient multiplied by K_{Ca}. In the above expression, C_r is equal to $[Ca^{2+}]_r/K_{Ca}$, where $[Ca^{2+}]_r$ is the intracellular calcium concentration at the resting potential.

IV. RESULTS

A. Experimental Data and Simulation

To produce sustained bursts that closely simulated typical experimental data from R15, We took a new time series of electric activity in Fig.4 based on that in Fig.3 by using Mathematica program before anything else. So we used a time series of electrical activity in Fig.4 instead of that in Fig.3 to simulate the bursting activity of neuron R15. The estimated parametric values that define the model are:

$C_m = 1$, $g_{fast} = 1000$, $g_{slow} = 18.2$, $g_K = 200$, $g_L = 10$, $V_{fast} = 60$, $V_{slow} = 140$, $V_K = -80$, $V_L = -60$, $V_m = -12$, $S_m = 5, V_h = -40$, $S_H = -6$, $V_d = -30$, $S_d = 10$, $V_n = 15$, $S_n = 15$, $\tau_h^* = 0.17$, $\tau_d^* = 0.5$, $\tau_n^* = 0.1$, $\lambda_f = 0.011$, $\sigma = 130$, $\rho = 6.5$, $C_r = 0.1$, $k_{Ca} = 0.48$, $a_h = 0.5$, $a_d = 0.5$, $a_n = 0$, and $K_{Ca} = 0.7$.

To reiterate, in this model the slow Ca^{2+} current is responsible for the slow wave that underlies the bursting, and the fast inward current together with the delayed rectifying K^+ current is responsible for generating the spike activity. There are altogether six dynamic variables, V, h, d, f, n, and $[Ca^{2+}]_i$. In this model, λ_f determines the burst periodicity, i.e., the smaller the values of λ_f, the longer the burst periodicity becomes. However, as shown in Eq.(2)(since the rate of closing is determined by $[Ca^{2+}]_i$) ρ also determines the burst periodicity, i.e., the smaller the value of ρ, the longer the burst periodicity becomes.

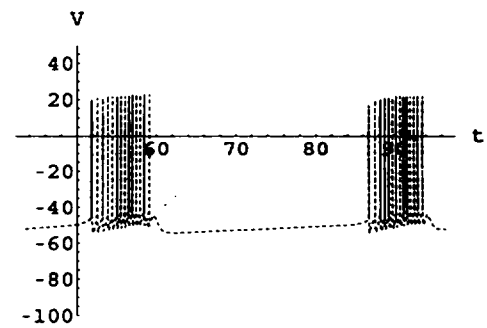

FIG. 4: A new series of electrical activity obtained by using Mathematica program.

Solutions of Eq.(1) - (7) require an estimation of the activation and inactivation time constants and the steady-state values of activation and inactivation at each membrane potential. A plot of the steady-state values of the m_∞, h_∞, d_∞, and n_∞ as a function of voltage is illustrated in Fig. 6.

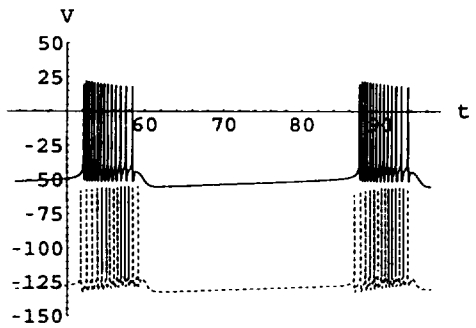

FIG. 5: A bursting pattern in the simulation of abdominal ganglion of Aplysia kurodai(solid lines) and a new series of electrical activity obtained by using Mathematica program(dashed curves).

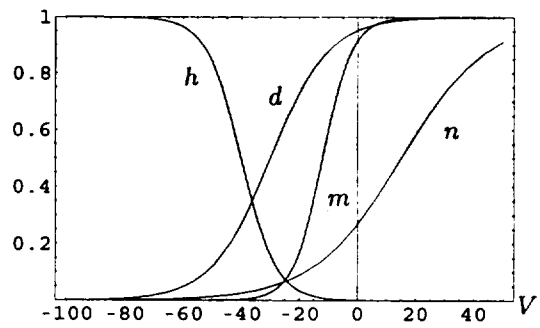

FIG. 6: Gating parameters of the model. Steady-state values of the gating variables(m_∞, h_∞, d_∞, and n_∞) plotted vs. potential

B. Membrane Currents and Time Series of Electrical Activity

Membrane currents contributing to the electrical activity was shown in Fig.7. Top panel illustrates a burst generated with the same parameters as in Fig.5, but it was shown on an expanded time scale. The large-amplitude currents(the fast inward current I_{fast}, the slow Ca^{2+} current I_{slow}, the delayed rectifying K^+ current I_K, and the leak current I_{leak}) contributing to the spikes during a burst are plotted below the membrane potential on the same time scale. The gating

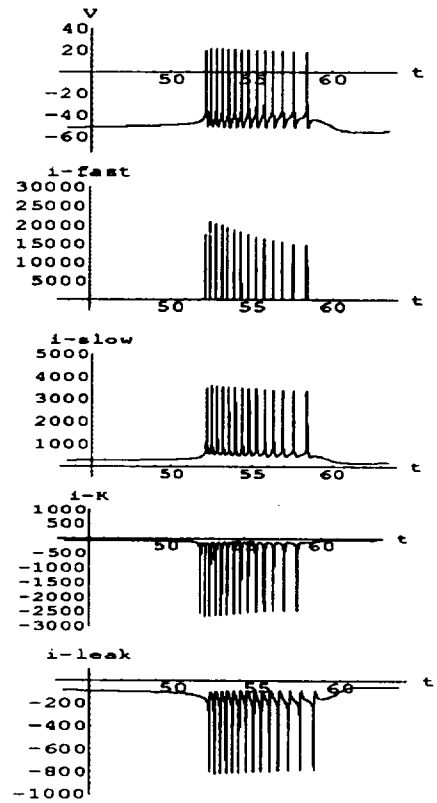

FIG. 7: Membrane currents contributing to the electrical activity. Top panel illustrates a burst generated with the same parameters as in Fig.5, but it was shown on an expanded time scale. The large-amplitude currents contributing to the spikes during a burst are plotted below the membrane potential on the same time scale.

variables d(t), f(t), h(t), and n(t) which is a fraction of available Ca^{2+} channels at time t, are also plotted on the same time scale as the figures in Fig.8.

Fig. 9 shows the time series of $[Ca^{2+}]_i$ oscillation. Fig.10 also shows the time course of membrane potential V (solid lines) and $[Ca^{2+}]_i$ oscillation(Dashed lines) predicted by the Ca^{2+}-blockable Ca^{2+} channel model. Note that the burst simulated from this model has an appearance very similar to those observed in neuronal bursting. Note in

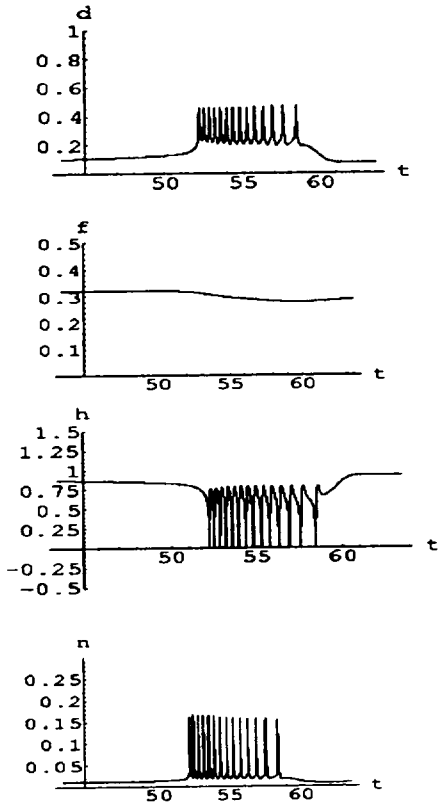

FIG. 8: The gating variables d(t), f(t), h(t), and n(t) which is a fraction of available Ca_{2+} channels at time t, are plotted on the same time scale as the figures in Fig. 6.

this figure that the shape of electrical burst is unaffected by the buffer strength ρ. However, as ρ decreases the burst period increases, and as the burst period increases the number of spikes increases. Although the shape of electrical bursting is not affected by ρ, the shape of $[Ca^{2+}]_i$ oscillations changes dramatically as ρ changes.

But the period of a burst becomes large as ρ decreases.[4] How ρ controls the burst periodicity can be understood from the kinematic scheme in E.(2). In this kinematic scheme, the period of the slow wave is determined by a parameter that affects the blocking and unblocking process of the Ca^{2+} channels. Note that the apparent rate of the blocking process is affected by the dynamic change of $[Ca^{2+}]_i$. This rate, in tern, is controlled by ρ which determines how fast $[Ca^{2+}]_i$ changes with varying membrane potential. Thus ρ is one of the factors that control the burst periodicity(via the rate of the change in $[Ca^{2+}]_i$.

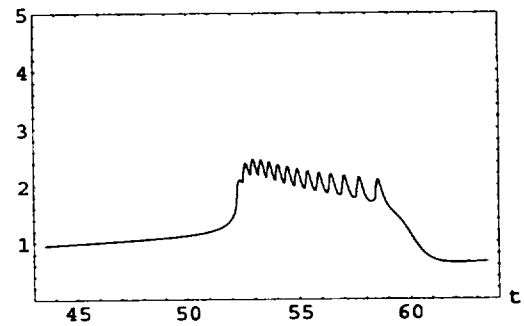

FIG. 9: $[Ca^{2+}]_i$ oscillation.

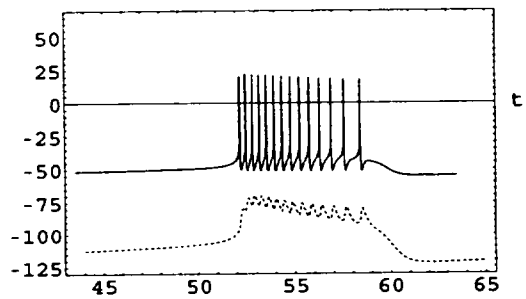

FIG. 10: The time series of electrical activity (solid lines) and the oscillation in the Ca^{2+} concentration, $[Ca^{2+}]_i$ (dashed curves) of a neuron based on the hypothesis of a Ca^{2+} - blockable Ca^{2+} channel. Note that the pattern of $[Ca^{2+}]_i$ oscillations is very different for different ρ values. The value of g_{slow} used for this computation is 18.2.

In this paper, using Mathematica program, we have simulated the bursting activity of neuron R15 in Aplysia kurodai recorded by J. H. Han at the Molecular Neurobiology Laboratory in SNU. The model based on Ca^{2+} -blockable Ca^{2+} channel was use to simulate

the activity of R15. Although the experimented and simulated results did not coincided, we saw the possibility to have better results in the future. Membrane currents and the oscillation in the Ca^{2+} contributing to the electrical activity were analyzed.

ACKNOWLEDGMENTS

The peresent study was partially supported by Cheju National University Research Fund, 2001. We are thankful to J. H. Han and Prof.B. -K. Kaang at SNU for giving us a good data and lots of information about Aplysia kurodai.

[1] C. C. Canavier, J. W. Clark, and H. Byrne, Journal of Neurophysiology **66**(No.6), 2107-2124 (1991).

[2] S. S. Demir,R. J. Butera, Jr., A. A. DeFranceschi, J. W. Clark, Jr., and J. H. Byrne, Biophysical Journal **72**, 579-594 (1997).

[3] C. C. Canavier, J. W. Clark, and J. H. Byrne, Biophysical Journal **57**, 1245-1251 (1990).

[4] T. R. Chay, Y. S. Fan,and Y. S. Lee,International Journal of Bifurcation and Chaos, **5(3)**, 595-635 (1995).

[5] C. -S. Lim, D. Y. Chung, and B. -K. Kaang, Mol. Cells, **7** (3), 399-407 (1997).

[6] E. R. Kandel, Cellular Basis of Behavior, W. H. Freeman Co., New York, NY, (1979).